Computational identification of potential multi-drug combinations for reduction of microglial inflammation in Alzheimer disease

Thomas J. Anastasio *

Computational Neurobiology Laboratory, Department of Molecular and Integrative Physiology, Beckman Institute, University of Illinois at Urbana-Champaign, Urbana, IL, USA

Like other neurodegenerative diseases, Alzheimer Disease (AD) has a prominent inflammatory component mediated by brain microglia. Reducing microglial inflammation could potentially halt or at least slow the neurodegenerative process. A major challenge in the development of treatments targeting brain inflammation is the sheer complexity of the molecular mechanisms that determine whether microglia become inflammatory or take on a more neuroprotective phenotype. The process is highly multifactorial, raising the possibility that a multi-target/multi-drug strategy could be more effective than conventional monotherapy. This study takes a computational approach in finding combinations of approved drugs that are potentially more effective than single drugs in reducing microglial inflammation in AD. This novel approach exploits the distinct advantages of two different computer programming languages, one imperative and the other declarative. Existing programs written in both languages implement the same model of microglial behavior, and the input/output relationships of both programs agree with each other and with data on microglia over an extensive test battery. Here the imperative program is used efficiently to screen the model for the most efficacious combinations of 10 drugs, while the declarative program is used to analyze in detail the mechanisms of action of the most efficacious combinations. Of the 1024 possible drug combinations, the simulated screen identifies only 7 that are able to move simulated microglia at least 50% of the way from a neurotoxic to a neuroprotective phenotype. Subsequent analysis shows that of the 7 most efficacious combinations, 2 stand out as superior both in strength and reliability. The model offers many experimentally testable and therapeutically relevant predictions concerning effective drug combinations and their mechanisms of action.

Keywords: microglia, neurodegeneration, systems biology, computational biology, polypharmacology

Introduction

Alzheimer Disease (AD) remains the leading neurological killer (www.alz.org). Currently there are no effective means to treat AD or even to slow its progression. As a neurodegenerative disease the pathological outcome of AD is death of neurons. For decades, research on AD has centered on the "amyloid hypothesis," according to which an over-accumulation of the

peptide amyloid-β (Aβ) causes neuron death (Hardy and Selkoe, 2002). New evidence continues to support a role for Aβ as a factor in AD (Hardy et al., 2014) but it also increasingly indicates that Aβ is not the only factor (Reitz, 2012; Skaper, 2012; Armstrong, 2014). Clinical, epidemiological, and laboratory evidence strongly implicates inflammation as a key component of AD pathogenesis (Griffin and Mrak, 2002; Von Bernhardi, 2007; Miklossy, 2008; Piazza and Lynch, 2009; Mandrekar-Colucci and Landreth, 2010; Johnston et al., 2011). That research suggests that Aβ, especially in the aged brain, can trigger a neurotoxic, inflammatory response and that pharmacological reduction of that response could be an effective way to treat AD.

A type of glial cell known as microglia mediates the inflammatory response in the brain (Ransohoff and Perry, 2009; Kettenmann et al., 2011). Microglia can express a number of different phenotypes in response to a wide range of stimuli including Aβ. Their physiology is extraordinarily complex. A recent computational model sought to characterize the responses to Aβ of microglia from young and old brains (Anastasio, 2014). That model provided new insights into microglial behavior and offered potential explanations for the observations that exposure to Aβ increases the production by young microglia of both pro- and anti-inflammatory mediators, and that old microglia tend to remain in a neurotoxic phenotype once they convert to it. The microglia model also identified certain cell-signaling pathways that could be instrumental in moving microglia away from a neurotoxic phenotype, but it did not explore the potential for drugs to influence those pathways.

The purpose of this paper is to use the microglia model to identify drugs, and specifically to identify drug combinations, that have the potential to reduce microglial inflammation in aged brains exposed to Aβ. As for the original microglia model, the *in silico* drug study presented here will exploit the synergistic strengths of two computer programming modalities, one imperative and the other declarative. Imperative programming, by far the more common modality, is designed for efficient computation while declarative programming is designed for computational analysis. The difference stems from the distinct nature of a statement in either modality. Basically, a statement in an imperative program is a command (e.g., add 3 and 3) but a statement in a declarative program is a declaration of a fact (e.g., 3 plus 3 can be replaced by 6). In an imperative program statements execute in the order in which they are listed, but in a declarative program a statement may execute or not. Consequently, in an imperative program statements are constrained to execute in only one order, while in a declarative program statements can execute in all possible orders.

The main benefit of a declarative programming environment is that it keeps track of the results of all of its different sequences of statement executions. This feature is what makes declarative programming inefficient compared with imperative programming, but it is also what makes the declarative modality so useful for analysis. Because a declarative program keeps track of its progress along all statement sequences it can be queried to obtain critical information, such as whether a specific result can ever occur, or whether a specific result can only occur if a different specific result occurs first, and so on. The main tools

for analysis in declarative programming are known as state-space search and temporal-logic model-checking (Huth and Ryan, 2004). These tools are invaluable for the analysis of complex processes, and they are being applied increasingly to complex biological processes (e.g., Fisher and Henzinger, 2007).
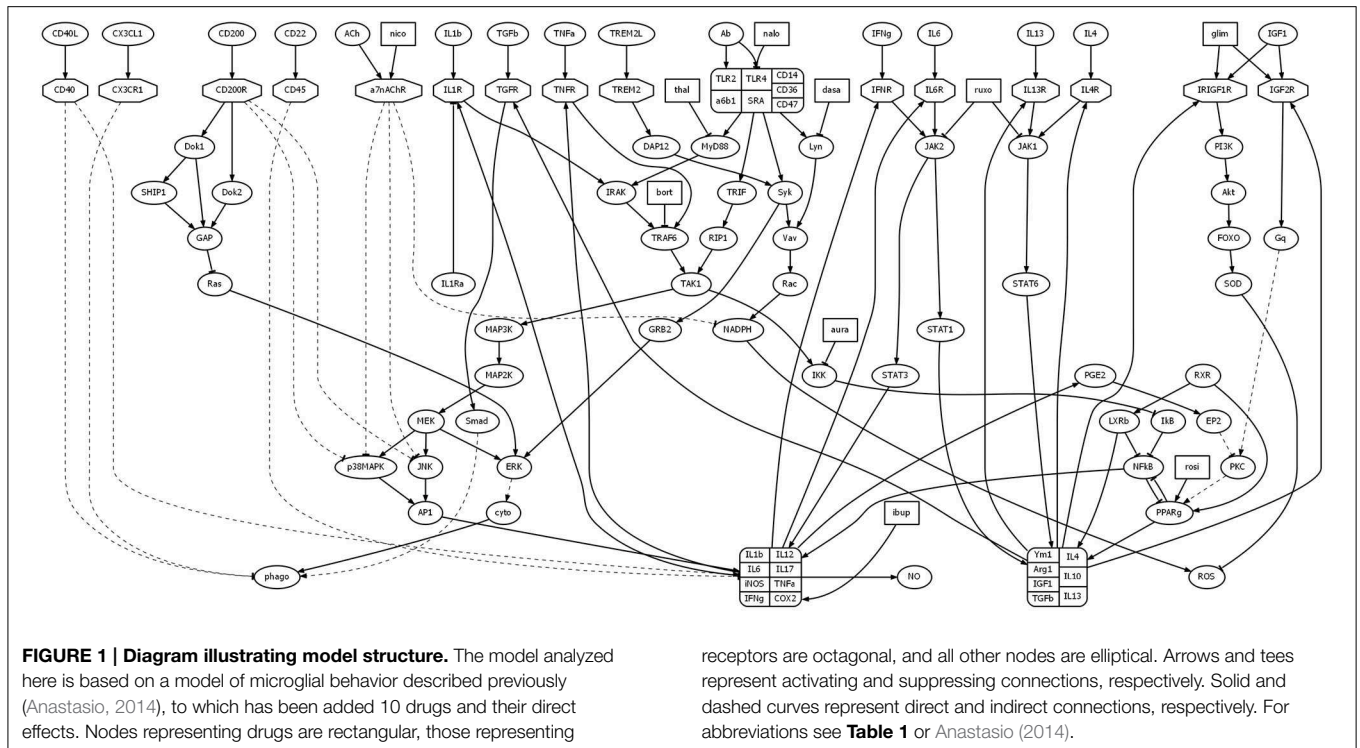
Here an imperative program implementing the microglia model will be used efficiently to screen for efficacy all 1024 combinations of 10 drugs. All of the 10 have been approved for use by the US Food and Drug Administration (FDA), and all are small-molecule drugs that could be taken orally and absorbed gastrointestinally and could cross the blood-brain barrier. Each of the drugs targets a different element (or pair of elements) of the model. All of them were identified using the DrugBank database (www.drugbank.ca). As such they are all well-known and widely used. The efficacy of each drug combination will be quantified by the extent to which it moves simulated microglia from a neurotoxic to a neuroprotective phenotype. Then a declarative program implementing the same microglia model will be used to analyze the mechanisms of action of the most efficacious drug combinations. As befits the complex nature of microglia, analysis of the model will reveal that complex sets of interactions mediate the effects of the efficacious drug combinations. The analysis will demonstrate how a computational model can be used to identify potential multi-drug strategies for the manipulation of complex biological processes, and will identify specific combinations of approved, small-molecule drugs that could reduce inflammation in the AD brain.

Methods

The goal of the study presented here was to computationally identify drug combinations with the potential to reduce microglial inflammation in AD. This study utilized a model of microglial behavior that was described in detail in a previous article (Anastasio, 2014). To this model were added 10 drugs. A schematic of the original model, along with the added drugs, is shown in **Figure 1**. Abbreviations of the names of the molecular species that are important for this study are listed in **Table 1** (abbreviations not listed in **Table 1** can be found in Anastasio, 2014). The immediate effects of each drug were set according to their main direct (proximal) effects as described in the literature, but the follow-on (distal) effects of the drugs are considered as modeling results and are described as such in Results. The first Subsection of Methods briefly summarizes the behavior of the microglia model, while the following two Subsections describe the imperative and declarative methods that were used to carry out the computational drug screens and analyses.

Microglia Model Behavior
The microglia model (Anastasio, 2014) represents the interactions between about 100 of the factors that are known from the literature to mediate the responses of microglia to Aβ and to other relevant stimuli. These factors are mainly molecular species (ligands, receptors, signaling molecules, transcription factors, etc.) but also include some cellular processes (e.g., phagocytosis). The microglia model is essentially a theory (albeit complex) about how microglia respond to different signals

FIGURE 1 | Diagram illustrating model structure. The model analyzed here is based on a model of microglial behavior described previously (Anastasio, 2014), to which has been added 10 drugs and their direct effects. Nodes representing drugs are rectangular, those representing receptors are octagonal, and all other nodes are elliptical. Arrows and tees represent activating and suppressing connections, respectively. Solid and dashed curves represent direct and indirect connections, respectively. For abbreviations see **Table 1** or Anastasio (2014).

present in their environment, which is the brain parenchyma. These signals are transduced, as in other cell types, via receptors, which activate cell-signaling pathways, which effect changes in microglial functions such as upregulation or downregulation of cytokines and other mediators, activation or inactivation of phagocytosis, and so on. A key feature of microglia, as of other immune cells, is that they respond to signals that they themselves produce. These autocrine interactions constitute positive and negative feedback loops through the operation of which microglia can change their phenotype.

Microglia can assume many different phenotypes (Ransohoff and Perry, 2009; Kettenmann et al., 2011). For modeling purposes it is convenient to define different phenotypes in terms of their production of cytokines and other mediators (growth factors, toxins, enzymes, etc.) and their expression of behaviors (mainly phagocytosis). The microglia model was focused on three phenotypes that are relevant to AD pathogenesis and have been studied mainly in normal mice and in transgenic mice that overproduce Aβ (for details and references see Anastasio, 2014). These three phenotypes can be referred to as mixed, neurotoxic, and neuroprotective.

The mixed phenotype occurs in "young" microglia (from mice less than 1 year old), in which secreted or membrane-bound signals from healthy neurons, such CX3CL1 (i.e., fractalkine), are present. When young microglia are exposed to Aβ, or to other inflammatory stimuli such as LPS, they increase their production of pro-inflammatory cytokines and toxins (as exemplified by IL1β and ROS, respectively), but also increase their production of anti-inflammatory cytokines (as exemplified by IL4) and become phagocytic. The microglia model explained this by invoking

the idea of an "autocrine bridge," over which transcriptional drive could effectively "cross" from the pro- to the anti-inflammatory "side." This occurred in the following way. Aβ (or LPS) activates the TLR complex, which initiates a signaling cascade that activates NFκB, which in turn upregulates a set of pro-inflammatory cytokines including IFNγ. IFNγ then activates the IFNR in an autocrine fashion, which activates JAK2/STAT1, which in turn upregulates a set of anti-inflammatory cytokines and other mediators including TGFβ. TGFβ then activates Smad, which in turn contributes to the activation of phagocytosis. This mixed, pro-and-anti-inflammatory phenotype is on the whole beneficial because phagocytic microglia clear Aβ, but its beneficial aspects do not occur unless the pro-to-anti-inflammatory bridge is crossed. The pro-to-anti-inflammatory bridge can be crossed by IFNγ or IL6, or potentially by other cytokines that signal via JAK2/STAT1, but removal of STAT1 severely dysregulates this mechanism.

The neurotoxic phenotype occurs in "old" microglia (from mice greater than 1 year old), in which signals from healthy neurons are absent. When old microglia are exposed to Aβ together with other inflammatory stimuli such as LPS, they increase their production of pro-inflammatory cytokines but decrease their production of anti-inflammatory cytokines and become non-phagocytic (Piazza and Lynch, 2009). The microglia model explained this by hypothesizing that a mutually antagonizing interaction between NFκB and PPARγ, which occurs in macrophages, also occurs in microglia. With this mutually antagonizing mechanism in place, the loss of healthy neuronal signals in old microglia combined with exposure to both Aβ and LPS pushed NFκB up higher than in the mixed

TABLE 1 | Abbreviations.

Names	Abbreviations	Elements
Acetylcholine	ACh	ACh
Adaptor protein 1	AP1	AP1
Alzheimer Disease	AD	n/a
Amyloid-β	Aβ	Ab
Auranofin	n/a	aura
α-7 Nicotinic acetylcholine receptor	α7nAChR	a7nAChR
Bortezomib	n/a	bort
c-Jun N terminal kinase	JNK	JNK
Cluster of differentiation #	CD#	CD#
Cytochrome C oxygenase 2	COX2	COX2
Cytoskeleton	n/a	cyto
Dasatinib	n/a	dasa
E prosthanoid receptor 2	EP2	EP2
Extracellular signal-related kinase	ERK	ERK
Fractalkine	CX3CL1	CX3CL1
Glimepiride	n/a	glim
G protein q	Gq	Gq
Ibuprofen	n/a	ibup
IL1 receptor-associated kinase	IRAK	IRAK
Inhibitor of κ B kinase	IKK	IKK
Insulin-like growth factor 1	IGF1	IGF1
Insulin-like growth factor 2 receptor	IGF2R	IGF2R
Insulin receptor and insulin-like growth factor 1 receptor	IRIGF1R	IRIGF1R
Interferon γ	IFNγ	IFNg
Interleukin 1-β	IL1β	IL1b
Interleukin #	IL#	IL#
Janus kinase #	JAK#	JAK#
Lipopolysaccharide	LPS	LPS
Liver tyrosine kinase	Lyn	Lyn
Myeloid differentiation primary response protein	MyD88	MyD88
Naloxone	n/a	nalo
Nicotine	n/a	nico
Nicotinamide adenine dinucleotide phosphate (reduced)	NADPH	NADPH
Nitric oxide	NO	NO
Non-steroidal anti-inflammatory drug	NSAID	n/a
Nuclear factor κ B	NFκB	NFkB
Peroxisome proliferator-activated receptor γ	PPARγ	PPARg
Phagocytosis	n/a	phago
Prostaglandin E 2	PGE2	PGE2
Protein 38 mitogen-activated protein kinase	p38MAPK	p38MAPK
Protein kinase C	PKC	PKC
Reactive oxygen species	ROS	ROS
Receptor-interacting protein 1	RIP1	RIP1

(Continued)

TABLE 1 | Continued

Names	Abbreviations	Elements
Rosiglitazone	n/a	rosi
Ruxolitinib	n/a	ruxo
Signal transducer and activator of transcription #	STAT#	STAT#
Sma protein from *Drosophila*	Smad	Smad
Spleen tyrosine kinase	Syk	Syk
Thalidomide	n/a	thal
Toll-like receptor #	TLR#	TLR#
Toll/interleukin 1 receptor (TIR)-domain-containing adaptor-inducing interferon β	TRIF	TRIF
TNF receptor-associated factor 6	TRAF6	TRAF6
Transforming growth factor β	TGFβ	TGFb
Transforming growth factor-associated kinase 1	TAK1	TAK1
Triggering receptor expressed on myeloid cells 2 ligand	TREM2L	TREM2L
Tumor necrosis factor α	TNFα	TNFa
Vav guanine nucleotide exchange factor	Vav	Vav

The name of each molecular species is listed along with its abbreviation and the name of the model element that represents it. Since the programming languages do not allow Greek characters they are replaced with lower-case Roman letters in model element names. To further distinguish model element names from actual molecule names they are rendered in monotype *font. The # symbol in abbreviations or model element names stands for an arbitrary integer number. Abbreviations or model element names are not applicable (n/a) to items that are, respectively, not abbreviated in the text or do not appear in the model.*

phenotype, and that in turn pushed PPARγ down to the point where it caused downregulation of anti-inflammatory mediators. The downregulated factors included TGFβ, which was not then high enough to promote phagocytosis. The neurotoxic phenotype is damaging to neurons because of high levels of pro-inflammatory cytokines and ROS, low levels of anti-inflammatory cytokines and other factors that support neuronal maintenance, and lack of Aβ clearance through microglial phagocytosis.

A key aspect of the mixed phenotype is that many but not all anti-inflammatory mediators are upregulated. Notable among those not upregulated is IGF1 (Butovsky et al., 2005). In the model this occurs because STAT1 upregulates most anti-inflammatory mediators but downregulates IGF1. A central feature of the model is autocrine interaction, through which each pro-inflammatory cytokine can upregulate itself and other pro-inflammatory cytokines. Because the cytokines upregulated by pro-inflammatory cytokines include IFNγ (and IL6), a pro-inflammatory cytokine can even upregulate certain anti-inflammatory factors. In contrast, an anti-inflammatory factor cannot, in the model, upregulate pro-inflammatory cytokines. While an anti-inflammatory factor can upregulate itself and most other anti-inflammatory factors, it cannot upregulate IGF1 when STAT1 has been activated. Otherwise, an anti-inflammatory

factor such as IL4 (or IL13) can temporarily upregulate IGF1 via STAT6 but, in the model, IGF1 must then activate its own signaling pathway via Gq in order to maintain a high level. Failure to do so leaves IGF1 vulnerable to STAT1.

Unlike the other anti-inflammatory mediators, IGF1 can downregulate pro-inflammatory cytokines. It accomplishes this essentially by reversing the transcriptional pattern that underlies the neurotoxic phenotype in the model. Specifically, IGF1 can drive up PPARγ, which then drives down NFκB, and this causes downregulation of pro-inflammatory cytokines along with upregulation of anti-inflammatory mediators. However, this beneficial influence of IGF1 is tenuous because IGF1 cannot depend on other anti-inflammatory mediators but must activate its own signaling pathway in order to maintain a high level. According to the model, the neurotoxic phenotype is persistent because microglia have only one mechanism available to escape it, but that mechanism requires sustained IGF1 expression, and that cannot occur through synergism with other pathways but depends on a single pathway that is initiated by IGF1 itself signaling though IGFR and Gq. In the model, movement away from the neurotoxic phenotype depends entirely on activation this pathway.

It is possible experimentally to reduce a pro-inflammatory microglial response, to restore Aβ phagocytosis, and to increase IGF1 expression using initially high levels of anti-inflammatory cytokines such as IL4, IL10, and IL13 (Butovsky et al., 2005; Koenigsknecht-Talboo and Landreth, 2005). In the model this phenotype can be produced though initial increase in IGF1 itself. It can also be produced through initial increase in IL4, or other anti-inflammatory cytokines that signal via JAK1/STAT6, but only if IGF1 subsequently maintains its own high level by activating Gq. In the model this phenotype is characterized by low levels of pro-inflammatory cytokines, high levels of anti-inflammatory cytokines (including IGF1), and phagocytosis of Aβ. This phenotype can be reached even from the neurotoxic phenotype provided that IGF1 activates its pathway through Gq. This microglial phenotype is considered neuroprotective because it would not damage neurons with high levels of pro-inflammatory cytokines or ROS, and it would clear Aβ and other debris through phagocytosis while it supports neural repair through secretion of growth factors and other proteins such as enzymes mediating cytoskeletal remodeling (see also Discussion).

In the model, the phenotype reached from the neurotoxic phenotype due to activation of IGF1/IGFR/Gq has ROS reduced from the high to the baseline level. For the purposes of the computational drug-combination screen presented here, the fully neuroprotective phenotype will have low ROS in addition to low pro-inflammatory cytokines, high anti-inflammatory mediators including IGF1, and a high level of Aβ phagocytosis. The goal of the computational screen is to identify which combinations of 10 approved drugs have the greatest potential to move microglia from the neurotoxic to the fully neruoprotective phenotype, and then to analyze the mechanisms of action of the most efficacious combinations. This is accomplished using data-driven computational models implemented in two different programming environments.

Data-driven Modeling Framework

The original model, on which this computational drug-combination screen is based, is a model of the signaling system by which microglia adjust their phenotype according to changes in the brain's microenvironment. The microglia system model is entirely data driven in that all of the interactions represented in it are based directly on the results of experiments as reported in the primary literature. These results were obtained using molecular and cellular biology techniques (gel electrophoresis, immunohistochemistry, phagocytosis assay, etc.) that provide relative measures of expression and/or activity and are useful for making statistical comparisons, but do not provide accurate measures of quantities such as concentrations or reaction rates. For the purposes of modeling it is therefore appropriate to quantize available data into a set of discrete integer levels. In establishing the framework for the microglia system model, the data were used to determine both the structure of the system and its overall input/output behavior (also called the model truth table; see below).

Model structure was determined from studies of microglia signaling pathways. For example, using a combination of immunological receptor-blocking, gel electrophoreses, immunohistochemistry, and *in vitro* binding assay, fibrillar Aβ was shown to activate a microglial receptor complex that includes TLR2, TLR4, and CD14, leading to phosphorylation of the tyrosine kinases Lyn and Syk, which in turn phosphorylate Vav (Combs et al., 1999; Reed-Geaghan et al., 2009). The structure of the original microglia model was built up using these and many similar results. To the original model were added proximal drug effects. For example, using a combination of immunoprecipitation and gel electrophoreses, the drug dasatinib was shown to block phosphorylation of Lyn (Nam et al., 2007).

The overall input/output behavior of the microglia system was determined from studies of the responses of microglia to the stimuli Aβ or LPS, or to high levels of various mediators (e.g., IFNγ). For example, using superoxide and *in vitro* phagocytosis assays, microglia from young mice were shown to respond to fibrillar Aβ by increasing both ROS production and phagocytosis (Wilkinson et al., 2006). These and many other similar findings were used to compose a system "truth table," which showed the effects of manipulating the levels of certain elements, designated as input elements, on the levels of certain other elements designated as output or endpoint elements. The input elements included Aβ and LPS while the output or endpoint elements included IL1β, IL4, IGF1, ROS, and phagocytosis. For the truth table, inputs such as Aβ and LPS were treated as binary (absent or present, 0 or 1), while naturally occurring molecules (e.g., IL1β or IL4) were assigned the integer levels of 5, 3, or 7 for baseline, low, or high, respectively, where low and high indicate observed, statistically significant increases or decreases from baseline, respectively. The truth table represented the findings with which the computational model had to agree.

Model structure dictated which model elements could influence with other elements and the polarity of that influence (activation or suppression), but these constraints left open many options for computationally describing how each element responded to its inputs from the other elements. The

parsimonious approach taken in model creation started by setting the absolute strengths of all connections to 1 (+1 for activating connections, −1 for suppressing connections). Then the functions that determine the expression/activation level (level function) for each element were set so that overall model behavior agreed with the truth table. This trail-and-error process involved complex interactions more so that simpler interactions. Thus, elements that receive input from 1 other element take the same level as their single input element. Elements that receive input from 2 or 3 other elements either take the maximal input or take sums and/or differences between the inputs (differences, like all other levels in the model, are bound from below at 0). Only about 15% of the elements in the original microglia model received more than three inputs. Their level functions were constructed in terms of specific input patterns. The more complicated level functions could depend on the values of inputs relative to each other or to preset threshold values, and could also involve saturation values that bound the level from above. An effort was made to keep the level functions as simple as possible while forging agreement between the model and the data-derived truth table (for further details see Anastasio, 2014).

The names of the model elements correspond to the usual abbreviations for the molecules they represent (with a few corresponding to cellular processes). Model element levels are constrained to take integer values in the range [0, 10]. To distinguish model elements from actual molecules (or cellular processes) their names are written in monotype font (see **Table 1**). The name of the original model of the behavior of microglia in the AD brain is ADMICRO. The name of this model augmented to include the effects of 10 drugs is ADMICRODRUGS. These computational models are instantiated as computer programs. Like ADMICRO, there are two versions of ADMICRODRUGS, one written in an imperative language and the other written in a declarative language.

Imperative Programming and Simulation
The imperative programming language used in this computational study is MATLAB™. MATLAB is designed for highly efficient computations, especially those that can be organized as matrix computations (the name "MATLAB" is short for "matrix laboratory"). MATLAB was used here to instantiate the ADMICRODRUGS model, to run repeated simulations of it, to perform the computational drug-combination screen, and to sort the results of the screen in order to remove redundancies.

In the MATLAB version all model elements are represented as integer variables, and all level functions assign integers in the range [0, 10] to their associated variable. For example, IL1b equals 7 when its level function has assigned it that level. To facilitate comparisons, the structure of the MATLAB program was made more similar to the Maude program (see next Subsection) by making all of its level functions conditional and placing them all within a while loop. The condition for any level function is satisfied if its execution would change the value of its associated variable, in which case the variable is updated and an update flag is set. The while loop continues as long as the update flag is set. What this means is that whenever a variable is updated, all level functions must be checked again to determine

whether any of their variables could now also change value. The while loop terminates when no further updates can be made. The MATLAB version did terminate for all of the input configurations represented in the truth table.

An ancillary MATLAB program automatically ran simulations of the MATLAB version of ADMICRODRUGS starting from each input configuration, collected the terminal state endpoint values, and computed the error between model and observed endpoints over the entire truth table. This ancillary program was used efficiently to evaluate trial-and-error changes in level functions during model creation (see previous Subsection). A terminal state of critical importance for this study is the neurotoxic state (i.e., phenotype; see Subsection Microglia Model Behavior). This state is reached in old microglia from the input configuration that includes both Ab and LPS (i.e., the neurotoxic input configuration). That input configuration is the one from which the drug-combination screen began. Another ancillary MATLAB program first constructed the matrix of all possible combinations of the 10 drugs screened in this study, ran a simulation for each combination starting from the neurotoxic input configuration to find the terminal state endpoint values for that combination, computed the percent efficacy of each combination, and then removed redundancies. The percent efficacy is a measure of the closeness of an endpoint pattern to the neuroprotective pattern, expressed as a percentage (see Results). A redundancy is a specific combination of drugs that is not more effective than a combination of the same drugs minus one or more of them. Determination of drug-combination efficacies and removal of redundancies was facilitated using matrix manipulations implemented in MATLAB.

Declarative Programming and Analysis
The declarative programming language used here is Maude (Clavel et al., 2007). Maude is designed to represent (i.e., model) and analyze complicated systems. A Maude model of a system is considered to be a module (the name "Maude" is derived from the word "module"). A module has an underlying algebra, which is composed of sorts (i.e., things) and operators (i.e., things done to things). The declarations in a Maude program are then based on this underlying algebra. Maude was also used here to instantiate the ADMICRODRUGS model and to analyze the model using state-space search and temporal-logic model checking.

In the Maude version of the model all elements are represented as operators that assign an integer (i.e., a sort) in the range [0, 10] to the level of that element. For example, IL1b(7) is an operator that assigns the integer 7 to the level of IL1b. Each declaration in the Maude program specifies the level function for an element in terms of the operators representing its inputs. In Maude there are two types of declarations: equations and rules. Applicable equations must execute but applicable rules may execute or not. This allows Maude to execute applicable rules in all possible orders thereby constructing the tree of all possible system states reachable given the rules (each branch is a different trajectory). Maude can search the tree for states of interest (i.e., state-space search) or can determine temporal relationships between states (i.e., temporal-logic analysis). In ADMICRODRUGS, as in ADMICRO, the level functions that

mediate the autocrine interactions (i.e., those that determine the levels of the receptors for the cytokines and other mediators that the microglia themselves produce) are expressed as rules, while all other interactions are expressed as equations. Thus, Maude determines all of the system states reachable through autocrine interactions in the model.

In the Maude version, as in the MATLAB version, all level functions are conditional, but unlike the MATLAB version the conditions are checked in arbitrary order in the Maude version (this is due to the essential difference between imperative and declarative programs). Like the MATLAB version the Maude version terminates for all input configurations but, unlike the MATLAB version, the Maude version reaches more than one terminal endpoint state for some input configurations. In all cases, for all input configurations and for all drug combinations tested, one Maude terminal endpoint state matched the single MATLAB terminal endpoint state. This signified that the two versions could implement the same computation and ensured that the results were not corrupted by programming error. In addition to providing a crosscheck, the Maude version was also used to analyze the mechanisms by with the efficacious drug combinations reduced neurotoxicity in the model.

Results

The results focus on the effects in the model of administration of 10 drugs alone and in all possible combinations. These drugs are, in alphabetical order, auranofin, bortezomib, dasatinib, glimepiride, ibuprofen, naloxone, nicotine, rosiglitazone, ruxolitinib, and thalidomide. All of these drugs are small-molecule and FDA approved (see also www.drugbank.ca). As small-molecules they can potentially cross the blood-brain barrier and exert their effects on microglia. Eight of the ten drugs normally are administered orally. The two exceptions are bortezomib and naloxone. Bortezomib is currently administered intravenously but oral forms of bortezomib are currently in clinical trial (Lawasut et al., 2012). Naloxone can be administered by various routes including orally, although the bioavailability of orally administered naloxone is low (Smith et al., 2012).

Thalidomide is a known teratogen but it has been re-approved by the FDA for limited use (Matthews and McCoy, 2003). Thalidomide reduces the level of MyD88 both by downregulating MyD88 mRNA expression and by increasing degradation of MyD88 by the proteasome (Noman et al., 2009). Bortezomib inhibits the proteasome as a main effect, but it also induces proteasome-independent degradation of TRAF6 (Fang et al., 2012). Thus, bortezomib and thalidomide both reduce inflammation by reducing signaling over inflammatory pathways. When used in conjunction, as they sometimes are clinically (Wang et al., 2014), bortezomib would lessen but not eliminate the anti-inflammatory effects of thalidomide by inhibiting the proteasome.

Naltrexone and naloxone, which block opioid receptors, and an isomer of naloxone that does not block opioid receptors, all act as antagonists of TLR4 (Hutchinson et al., 2008). The benefit of using the non-opioid isomer of naloxone is that it can block TLR4 and reduce inflammation but not block the analgesic effects of

opioids. While the opioid and the non-opioid naloxones both can inhibit TLR4 signaling, the non-opioid naloxone does not also inhibit TLR2 signaling (Lewis et al., 2012). Because of its reduced side effects the model incorporates the non-opioid, rather than the opioid, isomer of naloxone. Both TLR2 and TLR4 signal via Lyn and Syk. Dasatinib blocks activation (i.e., phosphorylation) of sarcoma kinases including Lyn (Nam et al., 2007); dasatinib does not block Syk because it is not a sarcoma kinase (McDonald et al., 1997; Combs et al., 1999).

Nicotine inhibits Aβ-induced microglial ROS production by preventing the activation of NADPH (Moon et al., 2008). This ROS suppression by nicotine was prevented by blockers of the α7nAChR. Ibuprofen, a well-known NSAID and COX2 inhibitor, can reduce inflammation, microglial activation, and AD deposits in AD-transgenic mice but its efficacy is age dependent (Lim et al., 2000; Yan et al., 2003; Sung et al., 2004). Rosiglitazone is a dose-dependent agonist of PPARγ that has known anti-inflammatory properties (Loane et al., 2009). Auranofin inhibits IKK (Jeon et al., 2000, 2003), while ruxolitinib inhibits both JAK1 and JAK2 (Verstovsek, 2013). Glimepiride is an insulin secretagogue, which causes insulin release from the pancreas (Campbell, 1998). Glimepiride is known to have anti-inflammatory properties (Ingham et al., 2014). All of these drugs directly target specific model elements.

The drugs are evaluated in terms of their effects on model behavior when it is started from the old initial condition. In this case, ACh, CD22, CD200, CX3CL1, and TREM2L, which represent secreted and/or membrane-bound substances produced by young, healthy neurons, are all absent (level 0), and the inflammatory stimuli Ab and LPS are both present (level 1). The effects are quantified in terms of the changes they make in the levels of a set of five key elements designed as endpoint elements. The endpoint elements are IL1b, ROS, phago, IL4, and IGF1, which represent, respectively, pro-inflammatory cytokines, toxins, phagocytosis, anti-inflammatory cytokines, and an anti-inflammatory factor of singular importance in the model (see also Anastasio, 2014). In all model terminal states the endpoint elements take one of three levels, which are 5, 3, and 7, corresponding to base, low, and high. In the absence of any intervention, the old initial state, with Ab and LPS both present, leads to the neurotoxic terminal state (i.e., phenotype) in which pro-inflammatory cytokines are high, ROS is high, anti-inflammatory factors are low, and phago is low. This can be expressed succinctly using Maude operators: in the old case with Ab(1) and LPS(1) the terminal state has IL1b(7), ROS(7), phago(3), IL4(3), and IGF1(3).

The neurotoxic endpoint pattern and many other reference endpoint patterns are listed in **Table 2**. The two most important are the neurotoxic pattern (**Table 2**, Row 6) and the neuroprotective pattern (**Table 2**, Row 7), because the efficacy of any drug combination was judged by its ability to move the microglia from the neurotoxic to the neuroprotective phenotype. Expressed as vectors, the neurotoxic and neuroprotective endpoint levels are [7 7 3 3 3] and [3 3 7 7 7], respectively. Then the efficacy of any single drug or drug combination was quantified by how much it moved the endpoint vector (as moving a needle on a dial) from the neurotoxic to the neuroprotective

TABLE 2 | Model endpoints from specific start conditions with no drugs or with single drugs.

Row	Condition	IL1b	ROS	phago	IL4	IGF1
1	Young microglia, AB(0), LPS(0), and no drugs (baseline)	5	5	5	5	5
2	Young microglia, AB(1), LPS(0), and no drugs (mixed)	7	7	7	7	3
3	Young microglia, AB(0), LPS(1), and no drugs (mixed)	7	7	7	7	3
4	Young microglia, AB(0), LPS(0), TNFaini(8), and no drugs	7	5	7	7	3
5	Old microglia, AB(0), LPS(0), and no drugs	7	5	3	7	3
6	Old microglia, AB(1), LPS(1), and no drugs (neurotoxic)	7	7	3	3	3
7	Old microglia, AB(1), LPS(1), but effects reversed (neuroprotective)	3	3	7	7	7
8	Young microglia, AB(0), LPS(1), and thal(1)	5	7	5	5	5
9	Young microglia, AB(0), LPS(1), and bort(1)	5	7	5	5	5
10	Young microglia, AB(1), LPS(0), and nico(1)	5	5	5	5	5
11	Young microglia, AB(0), LPS(1), and nico(1)	5	5	5	5	5
12	Young microglia, AB(1), LPS(0), and ibup(1)	5	7	7	7	5
13	Young microglia, AB(0), LPS(1), and rosi(1)	5	7	7	7	5
14	old microglia, AB(0), LPS(0), and rosi(1)	5	5	7	7	5
15	Young microglia, AB(0), LPS(1), and aura(1)	5	7	5	5	5
16	Young microglia, AB(0), LPS(0), TNFaini(8), and ruxo(1)	7	5	5	5	5
17	Young microglia, AB(0), LPS(1), and glim(1)	5	5	7	7	5

The first seven rows list a set of reference phenotypes with no drugs (including mixed, neurotoxic, and neuroprotective). The following 10 rows list specific phenotypic modifications due to certain drugs administered singly. The abbreviation TNFaini *stands for the initial level of* TNFa.

vector, and this amount was expressed as a percentage (0% meant no movement or fully neurotoxic, while 100% meant maximal movement or fully neuroprotective). The efficacies of all single drugs and of all non-redundant drug combinations are listed in **Table 3**.

The Effects of Each Drug Administered Alone in the Model

In ADMICRODRUGS, each drug affects one or more targets, which are the elements of the original ADMICRO. Each drug alters the level of its direct target(s) in a manner that persists into the terminal state of the model. The follow-on effect of each drug also alters the levels of other elements, such as signaling-pathway and transcription-factor elements. Some single drugs may also alter the levels of the endpoint elements IL1b, ROS, phago, IL4, and IGF1. Note that the effects of the drugs on their direct targets are explicitly set according to experimental findings (see previous Subsection for references), but all follow-on effects can be considered as modeling results.

Thalidomide reduces the level of MyD88. It does that in part by increasing degradation of MyD88 by the proteasome, so it would be less effective in conjunction with bortezomib, the main effect of which is to inhibit the proteasome. In ADMICRODRUGS, thal is set to reduce the level of MyD88 by 2 if bort is absent but only by 1 if bort is present. By reducing the level of MyD88 in the model, thal impairs the MyD88-initiated signaling that results in activation of transcription factor NFkB, but only in young microglia. For example, thal by itself is effective in young microglia challenged by LPS. In the young case with Ab(0) but LPS(1) and without any intervention, the terminal state has MyD88(1), with pathway elements IRAK(7), TRAF6(7), TRIF(1), RIP1(1), and

TAK1(7), and transcription factors NFkB(7) and PPARg(5). The endpoint states are IL1b(7), ROS(7), phago(7), IL4(7), and IGF1(3) (**Table 2**, Row 3). With NFkB(7) and PPARg(5), the pro- and anti-inflammatory mediators (except for IGF1) are expressed at the high level, and ROS is high but phago is also high. If this initial state includes thal(1), then the terminal state has MyD88(0), IRAK(4), TRAF6(5), TRIF(1), RIP1(1), TAK1(5), NFkB(5), and PPARg(5), and the endpoint states are IL1b(5), ROS(7), phago(5), IL4(5), and IGF1(5) (**Table 2**, Row 8). With NFkB(5) and PPARg(5), the pro-inflammatory cytokines, including IFNg, are held at base, and this prevents the microglial system from crossing the IFNg autocrine bridge that causes upregulation of anti-inflammatory mediators (except for IGF1; note that IFNg autocrine-bridge crossing causes IGF1 downregulation in the model). Consequently phago is also held at base, although ROS still rises to high. Thus, in the young case with LPS(1), initial thal(1), by suppressing MyD88, prevents LPS from activating NFkB, which prevents upregulation of pro-inflammatory cytokines, and this is consistent with observation (Noman et al., 2009).

Although thal is effective by itself in young microglia challenged by LPS, its effectiveness is quite different in old microglia challenged by Ab and LPS, which leads to the neurotoxic state in the model. Among the non-endpoint elements, the unaltered neurotoxic state has MyD88(2), IRAK(8), TRAF6(8), TRIF(2), RIP1(2), TAK1(9), NFkB(9), and PPARg(3), and the endpoint states are IL1b(7), ROS(7), phago(3), IL4(3), and IGF1(3) (**Table 2**, Row 6). If the initial state includes thal(1), then the terminal state has MyD88(0), IRAK(6), TRAF6(7), TRIF(2), RIP1(2), TAK1(9), NFkB(9), and PPARg(3),

TABLE 3 | Model endpoints starting from the old initial condition with `Ab(1)` and `LPS(1)` and with drugs either singly or in specific combinations.

Row	aura	bort	dasa	glim	ibup	nalo	nico	rosi	ruxo	thal	IL1b	ROS	phago	IL4	IGF1	% effect
1	1										7	7	7	7	3	26
2		1									7	7	3	3	3	0
3			1								7	7	3	3	3	0
4				1							7	5	3	3	3	5
5					1						7	7	3	3	3	0
6						1					7	7	3	3	3	17
7							1				7	5	3	3	3	5
8								1			7	7	3	3	3	0
9									1		7	7	3	3	5	5
10										1	7	7	3	3	3	0
11	1								1		7	7	5	5	5	10
12						1			1		7	7	5	5	5	10
13	1					1					5	7	3	5	5	17
14	1			1	1						5	5	7	7	5	51
15		1					1				5	5	7	7	5	51
16		1			1		1				5	3	7	7	5	72
17	1	1					1				5	3	7	7	5	72
18		1			1		1				5	3	7	7	5	72
19		1	1								3	5	7	7	7	78
20		1	1				1				3	3	7	7	7	100

*The neurotoxic endpoint pattern, which proceeds from the old initial condition with `Ab(1)` and `LPS(1)` and with no intervention, is shown in **Table 2**, Row 6.*

and the endpoint states are `IL1b(7)`, `ROS(7)`, `phago(3)`, `IL4(3)`, and `IGF1(3)` (**Table 3**, Row 10). In the model, `thal` reduces `MyD88` to 0, and this slightly reduces the levels of `IRAK` to 6 and `TRAF6` to 7. However, `TRIF` provides a pathway through `RIP1` to `TAK1` that parallels `MyD88`, and `TRIF` and `RIP1` are unaltered by `thal`. Combined with `RIP1` at 2, `TRAF6` at 7 is still enough to drive `NFkB` to 9 and that pushes `PPARg` down to 3. With `NFkB(9)` and `PPARg(3)`, the pro- and anti-inflammatory mediators all assume their unaltered neurotoxic levels. Adding to its ineffectiveness by itself, `thal(1)` does not reduce `ROS` or enhance `phago` either. Thus, `thal` by itself is ineffective in old microglia in altering any of the endpoints from their neurotoxic levels.

Because high-dose bortezomib is cytotoxic, `ADMICRODRUGS` simulates a relatively low dose. In the model, `bort` is set to hold the level of `TRAF6` to `base` (rather than push `TRAF6` to `low`) under all circumstances in which `TRAF6` would exceed `base`, thereby reducing `TRAF6` activation. The effects of `bort` by itself are similar to those of `thal`. By itself, `bort` does not alter any of the neurotoxic levels of the endpoint elements in old microglia challenged by `Ab` and `LPS` in the model (**Table 3**, Row 2). In contrast, in young microglia challenged by `LPS` alone, `bort` holds all pro- and anti-inflammatory mediators (including `IGF1`) to `base` and also holds `phago` at `base` although `ROS` still rises to `high` (**Table 2**, Row 9). Thus, `bort` reduces the response of young microglia to `LPS` alone, but is ineffective by itself in combating the neurotoxic state induced in old microglia by `Ab` and `LPS` in the model.

To simulate the effects of nicotine, `nico` is set to activate `a7nAChR` to level 2, and this causes indirect inhibition of

`NADPH`, `JNK`, and `p38MAPK`. In the absence of any intervention, young microglia with initial `Ab(1)` or initial `LPS(1)` reach a terminal state that has `a7nAChR(1)`, `NADPH(2)`, `ROS(7)`, `JNK(7)`, `p38MAPK(7)`, `AP1(7)`, `NFkB(7)`, and `TNFa(7)`. If either initial state has `nico(1)` then the terminal state has `a7nAChR(2)`, `NADPH(1)`, `ROS(5)`, `JNK(5)`, `p38MAPK(5)`, `AP1(5)`, `NFkB(5)`, and `TNFa(5)`. Here `nico` raises `a7nAChR` to 2, which pushes `NADPH` down to level 1, and that pushes `ROS` down to the `base` level of 5. It also holds `JNK` and `p38MAPK` to 5. This keeps `AP1` at 5, at which level it cannot increase `NFkB`. This keeps all pro-inflammatory cytokines including `TNFa` and `IFNg` at the `base` level (of 5), and that prevents the autocrine-bridge crossing that would otherwise elevate anti-inflammatory factors (except `IGF1`) and in turn elevate `phago` (**Table 2**, Rows 1–3, 10 and 11). In that `nico` reduces activation of `NADPH`, `JNK`, and `p38MAPK` and blocks production of `ROS` and `TNFa` in young microglia challenged by `Ab` or `LPS`, the model is consistent with observation (Shytle et al., 2004; De Simone et al., 2005; Moon et al., 2008). The neurotoxic state has `a7nAChR(0)`, `NADPH(2)`, `ROS(7)`, `JNK(10)`, `p38MAPK(10)`, `AP1(10)`, `NFkB(9)`, and `TNFa(7)`. If the initial state includes `nico(1)`, then the terminal state, as in the previous case, has `a7nAChR(2)`, which pushes `NADPH` down to level 1, which pushes `ROS` down to level 5. Also, the initial `nico(1)` again holds `JNK`, `p38MAPK`, and `AP1` to the `base` level of 5, but that does not result in reduction of pro-inflammatory cytokines or augmentation of anti-inflammatory factors or `phago` because the level of `NFkB` is still at the `over` level of 9. Thus, `nico` reduces `ROS` from `high` to `base` but does not otherwise

alter the neurotoxic phenotype by itself in the model (**Table 3**, Row 7).

To simulate the non-opioid isomer of naloxone, `nalo` is set to block activation of `TLR4` by `Ab` or `LPS`, but not to block activation of `TLR2` by `Ab`. (Note that `LPS` specifically activates `TLR4`; Necela et al., 2008; Park et al., 2009.) Among the non-endpoint elements, the unaltered neurotoxic state has `TLR2(1)`, `TLR4(2)`, `MyD88(2)`, `IRAK(8)`, `TRAF6(8)`, `NFkB(9)`, and `PPARg(3)`. If the initial state includes `nalo(1)`, then the terminal state has `TLR2(1)`, `TLR4(0)`, `MyD88(1)`, `IRAK(7)`, `TRAF6(7)`, `NFkB(7)`, and `PPARg(5)`. `TLR2` is not sensitive to `LPS` but still responds to `Ab`, which drives `TLR2` to level 1 and then `TLR2` drives `MyD88` to level 1. This level of `MyD88` is enough to drive `IRAK`, `TRAF6`, and `NFkB` to the high level of 7, which is enough to keep the pro-inflammatory cytokines high, but not enough to drive `PPARg low`, so the `IFNg` autocrine bridge can be crossed. This drives up most of the anti-inflammatory mediators except `IGF1`. The result is `IL1b(7)`, `IL4(7)`, and `IGF1(3)` (**Table 3**, Row 6). The initial `nalo(1)` does not alter `ROS`, which stays high, nor does it alter `phago`, which stays low. Thus, `nalo` by itself increases some anti-inflammatory factors but not `IGF1`, nor does it decrease `ROS`, or decrease pro-inflammatory cytokines, or increase `phago` in the neurotoxic phenotype of the model.

To simulate the effects of dasatinib, `dasa` is set to block activation of `Lyn` by `TLR2` or `TLR4`, but to have no effect on `Syk`. In the absence of any intervention, the neurotoxic state of old microglial in the model has `Lyn(2)`, `Syk(2)`, `NADPH(2)`, and `ROS(7)`. If the initial state includes `dasa(1)` then the terminal state has `Lyn(0)`, `Syk(2)`, `NADPH(2)`, and `ROS(7)`. Both `Lyn` and `Syk` drive `Vav`. In the model, `Syk` at level 2 is enough to bring `Vav` and then `NADPH` to level 2 and that is enough to drive `ROS` to high even though `Lyn` is blocked by `dasa`. Thus, `dasa` by itself does not reduce `ROS` nor does it alter the levels of any of the other endpoint elements in the neurotoxic state of the model (**Table 3**, Row 3).

The effects of ibuprofen are represented in `ADMICRODRUGS` according to its well-known main mechanism: `ibup` is set to prevent the increase in `PGE2` due to `COX2`. The follow-on effects of `ibup` depend on age and inflammatory stimulants in a complex way. In the young case without intervention and with `Ab(1)` but `LPS(0)`, the terminal endpoint states are `IL1b(7)`, `ROS(7)`, `phago(7)`, `IL4(7)`, and `IGF1(3)`, and the terminal levels of some of the non-endpoint elements are `PGE2(7)`, `EP2(7)`, `PKC(0)`, `PPARg(5)`, and `NFkB(7)`. When this young initial state includes `ibup(1)` these terminal states are `IL1b(5)`, `ROS(7)`, `phago(7)`, `IL4(7)`, `IGF1(5)`, `PGE2(0)`, `EP2(0)`, `PKC(5)`, `PPARg(8)`, and `NFkB(4)` (**Table 2**, Rows 2 and 12). By inhibiting `COX2`, `ibup` blocks `PGE2` and subsequent `EP2` production, and the resulting disinhibition of `PKC` increases `PPARg`, which decreases `NFkB`. The result is a decrease in pro-inflammatory cytokines to the base level, retention of high levels of most anti-inflammatory cytokines and with an increase in `IGF1` to base, and no decrease in `ROS` but also no decrease in `phago`. However, in the old case with both `Ab(1)` and `LPS(1)`, which leads to the neurotoxic terminal state, `NFkB` is 9, `PPARg` is 3, and `ibup` has no effect

on model endpoints (**Table 3**, Row 5). If the neurotoxic state of the model does indeed reflect the microglial state in the aged and AD brain, as conjectured here (see Discussion), then these model attributes are consistent with experimental findings. They show that NSAIDs including ibuprofen are effective in reducing inflammation and (through phagocytosis) Aβ plaque formation in AD-transgenic mice, but only if chronic NSAID treatment is begun while the animals are still young (Lim et al., 2000; Yan et al., 2003; Sung et al., 2004).

To simulate rosiglitazone, `rosi` is set to strongly (but not fully) activate `PPARg`. If the young initial state has `LPS(1)` but `Ab(0)` and there is no intervention, then the terminal endpoint are `IL1b(7)`, `ROS(7)`, `phago(7)`, `IL4(7)`, and `IGF1(3)`, and the terminal level of `PPARg` is 5 and of `NO` is 7. If the initial state includes `rosi(1)`, which raises `PPARg` to 8, then `NO` falls to 5 and the terminal state has `IL1b(5)`, `ROS(7)`, `phago(7)`, `IL4(7)`, and `IGF1(5)` (**Table 2**, Rows 3 and 13). Thus, `rosi` brings the pro-inflammatory cytokines down to base and `IGF1` up to base, while `phago` and the other anti-inflammatory factors retain the high level. Although `ROS` is not reduced, `NO` is reduced. In the old case without inflammatory stimuli (i.e., `LPS` and `Ab` are both 0), the untreated terminal state has `IL1b(7)`, `ROS(5)`, `phago(3)`, `IL4(7)`, and `IGF1(3)` (**Table 2**, Row 5). Additionally `PPARg` is 5 and `NO` is 7. Including `rosi` in this case, which again raises `PPARg` to 8, again brings the pro-inflammatory cytokines down to base and `IGF1` up to base, and the other anti-inflammatory factors retain the high level. Additionally `phago` is increased to 7 while `NO` is decreased to 5 (**Table 2**, Row 14). In that `rosi` reduces `IL1b` and `NO` in the young case with `LPS(1)` and in the old case without any inflammatory stimulus, the model is consistent with experimental findings (Loane et al., 2009). Because the synergistic combination of `Ab` and `LPS` in the old case raises `NFkB` to 9, which pushes `PPARg` down to 3 despite `rosi`, `rosi` has no effect by itself on the neurotoxic state of the model (**Table 3**, Row 8).

To simulate auranofin, `aura` is set to hold `IKK` to 4 if `TAK1` is less than `over` but to 5 if `TAK1` reaches the `over` level. In both cases `aura` has some efficacy. Again, if the young initial state has `LPS(1)` but `Ab(0)` and with no intervention, then the terminal endpoints are `IL1b(7)`, `ROS(7)`, `phago(7)`, `IL4(7)`, and `IGF1(3)`, and among non-endpoints `IKK` and `NFkB` are both 7. If the initial state includes `aura(1)` then `IKK` and `NFkB` are both held at 4 and the terminal state has `IL1b(5)`, `ROS(7)`, `phago(5)`, `IL4(5)`, and `IGF1(5)` (**Table 2**, Rows 3 and 15). Thus, `aura` blocks the response of young microglia to `LPS` in the model, except that it does not reduce `ROS`. In that `aura` reduces the `LPS`-induced increases in `IKK` and `NFkB` in the model it is consistent with experimental findings (Jeon et al., 2000, 2003). Because `aura` acts directly on `IKK`, which activates `NFkB`, `aura` does have an effect by itself in reducing the severity of the neurotoxic state. Again, if the old initial state has `Ab(1)` and `LPS(1)` and there is no intervention then the neurotoxic terminal state occurs. It has endpoints `IL1b(7)`, `ROS(7)`, `phago(3)`, `IL4(3)`, and `IGF1(3)`, and the non-endpoints `IKK` and `NFkB` are both 9. If that initial state has `aura(1)` then `IKK` and `NFkB` are held at 5 and the endpoints

are `IL1b(7)`, `ROS(7)`, `phago(7)`, `IL4(7)`, and `IGF1(3)` (**Table 3**, Row 1). Thus `aura` by itself brings the model from the neurotoxic phenotype, which results in old microglia with `Ab(1)` and `LPS(1)`, to the mixed phenotype that results in young microglia with `Ab(1)` or `LPS(1)` but not both (**Table 2**, Rows 2 and 3).

To simulate ruxolitinib, `ruxo` is set to hold both `JAK1` and `JAK2` to the `base` level. In the young case with enhanced initial TNFa (`TNFaini(8)`) but with `Ab` and `LPS` both 0 and no other intervention, the model terminal state has endpoints `IL1b(7)`, `ROS(5)`, `phago(7)`, `IL4(7)`, and `IGF1(3)`. It also has `IL6(7)` and `TNFa(7)`, and `JAK1`, `JAK2`, and `STAT1` are all 7. If this initial state also includes `ruxo(1)` then `JAK1`, `JAK2`, and `STAT1` are reduced to 5, and the terminal state has endpoints `IL1b(7)`, `ROS(5)`, `phago(5)`, `IL4(5)`, and `IGF1(5)`, and also `IL6(7)` and `TNFa(7)` (**Table 2**, Rows 4 and 16). This is consistent with findings that ruxolitinib inhibits TNFα-induced JAK1/2 and STAT1 activation but does not significantly reduce TNFα-induced production of IL1β, IL6, and TNFα itself (Yarilina et al., 2012; Verstovsek, 2013). Although `ruxo` does not reduce pro-inflammatory cytokines in this case it shifts all anti-inflammatory factors to the `base` level, and this represents a reduction for all the anti-inflammatory factors except `IGF1`, which is actually augmented from `low` to `base` by `ruxo`. This last effect alone is recapitulated in the neurotoxic state, in which `ruxo` by itself does not alter the levels of any endpoint elements except for `IGF1`, which takes the `base` rather than the `low` level (**Table 3**, Row 9).

To simulate glimepiride, `glim` is set to raise the activation of `IRIGF1R` to level 7 and of `IGF2R` to level 6, to reflect findings that IGF2R is less sensitive to insulin than is the hybrid insulin-IGF1 receptor IRIGF1R (Fernandez and Torres-Aleman, 2012). Again, if the young initial state has `LPS(1)` but `Ab(0)` and there is no intervention, then the terminal endpoint states are `IL1b(7)`, `ROS(7)`, `phago(7)`, `IL4(7)`, and `IGF1(3)`, and additionally `TNFa(7)`. If this initial state includes `glim(1)` then the terminal endpoints are `IL1b(5)`, `ROS(5)`, `phago(7)`, `IL4(7)`, and `IGF1(5)`, and also `TNFa(5)` (**Table 2**, Rows 3 and 17). Thus `glim` decreases the levels of the pro-inflammatory endpoints and `ROS` from `high` to `base` but does not decrease the `high` level attained by `phago` and the anti-inflammatory factors except for `IGF1`, which is actually increased from `low` to `base`. In that `glim` opposes the LPS-induced increases in pro-inflammatory cytokines including `IL1b` and `TNFa`, the model is consistent with experimental observations in microglia (Ingham et al., 2014). Because `glim` fully activates `IRIGF1R` it also reduces `ROS` from `high` to `base` in the neurotoxic phenotype but, because `glim` does not fully activate `IGF2R`, it does not alter any other neurotoxic endpoint states by itself in the model (**Table 3**, Row 4).

Temporal-logic Analysis of Antagonistic Drug Combinations

Half of the drugs applied by themselves reduced the severity of the neurotoxic phenotype, with efficacies ranging from 5 to 26% (**Table 3**, Rows 1–10). The two most effective single drugs were `aura` (26% efficacy) and `nalo` (17% efficacy). There were three pairs of drugs that were actually less effective than one member of the pair alone. The drug `ruxo` reduced the efficacies of `aura` and of `nalo` (**Table 3**, Rows 11 and 12). Through its inhibition of both `JAK1` and `JAK2`, `ruxo` disrupts the autocrine interactions by which pro-inflammatory cytokines can drive up most anti-inflammatory mediators but drive down `IGF1`. The result is that `ruxo` prevents `aura` or `nalo` from driving up `IL4` and some other anti-inflammatory mediators, and in the case of `aura` it also prevents the increase in `phago` that is due in part to the increase in `TGFb`. However, `ruxo` prevents the neurotoxic decrease of `IGF1` that `aura` or `nalo` alone do not prevent but that `ruxo` does prevent by itself (**Table 3**, Row 9).

On its own, `aura` moves the neurotoxic phenotype in a neuroprotective direction by raising anti-inflammatory cytokines like `IL4` to `high` and also raising `phago` to `high`. With `aura` alone, temporal logic shows that `NFkB` never rises above `base` but `AP1` is always above `high`, and that leads to `high` expression of pro-inflammatory cytokines like `IL1b` and `IFNg`. Also `STAT1` eventually reaches `high`, which implies that `IL4` and `TGFb` are `high` but `IGF1` is `low`. In this way `aura` allows crossing of the autocrine bridge by which pro-inflammatory cytokines like `IFNg` raise the levels of anti-inflammatory factors like `IL4` and `TGFb` but lower the level of `IGF1`. The analysis also shows that with `aura` alone, `ERK` can still reach a level above `high` and this allows `TGFb` to drive `phago` to `high` in this case. With `aura` and `ruxo` together, `STAT1` does not eventually reach `high` because `ruxo` suppresses `JAK2`, so the rise in most anti-inflammatory mediators along with the fall in `IGF1` does not occur, but `NFkB` still never rises above `base`, so all the anti-inflammatory mediators (including `IGF1`) and `phago` stay at `base`.

The situation with `nalo` is similar. With `nalo` alone, `NFkB` does rise above `base` but never rises above `high`, so `NFkB` drives up the pro-inflammatory cytokines but `NFkB` never reaches the `over` level necessary to override the autocrine bridge. Therefore, as with `aura`, the autocrine bridge is crossed and `STAT1` eventually reaches `high` with `nalo` also, and drives up most anti-inflammatory cytokines including `IL4` and `TGFb` while it drives down `IGF1`. However, `nalo` does not allow `ERK` to rise above `high`, which it would need to do in this case to allow `TGFb` to drive up `phago`. With `nalo` and `ruxo` together, `STAT1` does not eventually reach `high` because `ruxo` suppresses `JAK2`, so the rise in the anti-inflammatory mediators such as `IL4` and `TGFb`, and the fall in `IGF1`, does not occur. Still, `NFkB` never rises above `high`, so the anti-inflammatory mediators as well as `phago` stay at `base`. Thus, `ruxo` thwarts both `aura` and `nalo` by suppressing `JAK2` (the suppression by `ruxo` of `JAK1` is less relevant here).

The third antagonistic drug pair is `aura` and `nalo`. Their interference can be explained by their respective effects on `ERK` and `NFkB`. In the signaling pathway leading from `Ab` and `LPS` stimulation, `nalo` works further upstream than `aura` by blocking `TLR4`. In consequence, `nalo` suppresses `ERK` but `aura` does not. In combination, `nalo` reduces the percent efficacy of `aura` alone to the level of `nalo` alone, but the endpoint pattern of the `aura` and `nalo` combination is different

from the pattern due to `nalo` alone (**Table 3**, Rows 1, 6, and 13). With `aura` and `nalo` together, `NFkB` is suppressed further than with either drug alone and never even reaches the `base` level. Having `NFkB` below `base` implies that pro-inflammatory cytokines like `IL1b` and `IFNg` are at kept at `base`, which prevents autocrine-bridge crossing and so further implies that anti-inflammatory factors like `IL4`, `TGFb`, and `IGF1` are kept at `base`. With `aura` and `nalo` together, unlike `aura` alone but as with `nalo` alone, the rise in `ERK` is suppressed and that causes `phago` to fall to `low` in this case. In all of the cases examined in this Subsection, which are `aura` alone, `nalo` alone, each separately combined with `ruxo`, or `aura` and `nalo` together without `ruxo`, `ROS` is not suppressed but reaches the `high` level. Although `nalo` antagonizes `aura`, and `aura` undoes some of the benefit of `nalo`, the `aura` and `nalo` combination is synergistic when `glim` is added to the mix (see next Subsection).

Temporal Logic Analysis of Synergistic Drug Combinations

There were 376 combinations with percent efficacies of 50% or greater, but the overwhelming majority of these were redundant in the sense that one or more drugs in the combination did not increase the overall efficacy of the combination. Removing all redundancies reduced the number of combinations with efficacies of 50% or greater to only seven (**Table 3**, Rows 14 to 20). Of all ten drugs, `glim` was the only drug present in all seven of the synergistically efficacious combinations. Temporal-logic analysis shows that `glim` by itself keeps `ROS` to the `base` level. While `glim` also helped keep `ROS` at or below `base` in all seven synergistic combinations, its contribution to efficacy was not limited to `ROS` reduction.

The drug `glim` greatly improves the efficacy (to 51%) of the `aura` and `nalo` combination in one of the two stable states associated with this combination (**Table 3**, Row 14). In addition to reducing `ROS`, `glim` allows `PPARg` to rise to the `over` level along the trajectory leading to the more efficacious state. This raises the level of anti-inflammatory factors such as `IL4` and `TGFb` to `high`, and this rise is self-sustaining in the stable state in which `STAT6` attains the `high` level. The effects of `nalo` on `ERK` allow `TGFb` to drive up `phago`. Due to the combination of `aura` and `glim`, `NFkB` is kept below `base` so the pro-inflammatory cytokines cannot rise above `base` and cannot drive `IGF1` below `base`.

There are three stable states associated with the combination of `glim` and `rosi`. The most efficacious of these has the same percent efficacy (of 51%) and endpoint pattern as the `aura`, `glim`, and `nalo` combination (**Table 3**, Rows 14 and 15), and the efficacious states of `aura/glim/nalo` and of `glim/rosi` are similar but occur via different mechanisms. Along its most efficacious trajectory, the combination `glim/rosi` works mainly by driving `PPARg` above `high`, which pushes `NFkB` below `base`. With these key transcriptions factors at those levels, the pro-inflammatory cytokines are held at `base` and cannot drive down `IGF1`, which also stays at `base`, but the other anti-inflammatory factors are driven `high`. The `glim/rosi` combination does not affect the `TLR2/TLR4` signaling pathway so `ERK` is allowed to rise and, in this case, that allows `TGFb`

to drive `phago` to the `high` level. Adding `nico` to the `glim/rosi` combination increases its efficacy to 72% (**Table 3**, Rows 15 and 16). The main contribution of `nico` to the `glim/nico/rosi` combination is to further reduce `ROS` by always keeping the level of `NADPH` less than 2.

Two other combinations have the same efficacy (of 72%) and the same terminal endpoint pattern as the `glim/nico/rosi` combination. These are the `aura/glim/nico` and the `nalo/glim/nico` combinations (**Table 3**, Rows 17 and 18). Two stable states are associated with `aura/glim/nico`. For both of them, due to `aura` and `glim`, `NFkB` never rises above `base`. In consequence, pro-inflammatory factors such as `IL1b`, and the anti-inflammatory `IGF1`, eventually settle at `base`. Due to the combined influences of `glim` and `nico`, `ROS` is held at `low` in both stable states. Along the more efficacious trajectory, an increase in `PPARg` above `high` drives `STAT6` to the `high` level, and that leads to sustained `high` expression of anti-inflammatory factors such as `IL4` and `TGFb`. Because `TLR2/TLR4` signaling is not disrupted by the `aura/glim/nico` combination, `ERK` eventually rises above `high`, and that allows `TGFb` to drive `phago` to the `high` level in this case.

There are also two stable states associated with the `nalo/glim/nico` combination, and the mechanism by which the more efficacious state occurs is similar to that of the `aura/glim/nico` combination with two small differences. First, because `nalo` blocks `TLR4` signaling, `ERK` is held below `high`, but that also allows `TGFb` to drive `phago` to `high` in this case. Second, `PPARg` eventually reaches `base` in both combinations, but that in conjunction with `STAT1` at `base` is enough to keep `IGF1` at `base` for the `nalo/glim/nico` combination. Otherwise, the mechanisms for keeping the pro-inflammatory cytokines at `base`, the anti-inflammatory factors (except `IGF1`) at `high`, and `ROS` at `low` are similar between these two combinations (**Table 3**, Rows 17 and 18).

The most efficacious combinations are `glim/ibup` and `glim/ibup/nico` (**Table 3**, Rows 19 and 20), and their mechanisms are the simplest. Both combinations are associated with only one stable state, as are each of `glim`, `ibup`, and `nico` separately. With `glim` by itself, `PPARg` rises to the `over` level but it does not stay there, while with `ibup` by itself `PPARg` eventually falls to `low`. However, with `glim` and `ibup` in combination, `PPARg` rises to `over` and stays there due to the rise in `Gq` by `glim` and the fall in `EP2` by `ibup`. By raising `Gq` to `high` this combination ensures sustained `high` expression of `IGF1`, which drives up the level of `PPARg`. When `PPARg` reaches the `over` level it drives `NFkB` `low`, and this configuration of these key transcription factors brings forth the expression pattern characteristic of the neuroprotective state in which all pro-inflammatory cytokines are `low` and all anti-inflammatory mediators, including `IGF1`, are `high`. With `glim/ibup`, `ERK` can still rise above `high` and that allows `TGFb` to drive `phago` to `high` in this case, and `glim` reduces `ROS` to `base`. All that separates this endpoint pattern from the fully neuroprotective pattern is that `ROS` is reduced all the way to `low` in the latter.

The `glim/ibup` combination just described has 78% efficacy (**Table 3**, Row 19). Adding `nico` to the mix raises

its efficacy to 100% (**Table 3**, Row 20). The combination `glim/ibup/nico` exhibits all the same mechanisms as the `glim/ibup` combination but it also keep `ROS` at `low` due to the activation by `nico` of the `a7nAChR`. Thus, in the model, microglia can be brought from the neurotoxic state to the fully neuroprotective state by a combination of `glim`, `ibup`, and `nico`.

Discussion

The key finding of this study is the identification of seven specific combinations of FDA-approved, small-molecule drugs that could potentially reduce microglial inflammation in the aged and AD brain (**Table 3**, Rows 14–20). Many lines of evidence indicate that the basal state of microglia becomes more inflammatory with age (for review see Wong, 2013). This chronic neuroinflammation is associated with higher levels of pro-inflammatory cytokines, and possibly also with higher levels of certain anti-inflammatory cytokines. The microglia model takes on this phenotype in the old case in the absence of `Ab` and `LPS` (**Table 2**, Row 5) due to the lack of `ACh`, `CD22`, `CD200`, `CX3CL1`, and `TREM2L`. These neuronal factors are associated with young, healthy neurons and they suppress microglial inflammation in the model. This is consistent with experimental findings (for references see Anastasio, 2014) with the possible exception of CX3CL1, findings for which are ambiguous. Some studies indicate that CX3CL1, also known as fractalkine, can partially suppress the pro-inflammatory response of microglia (Cardona et al., 2006), while other studies indicate that it can suppress phagocytosis of Aβ and partially enhance the pro-inflammatory response of microglia in transgenic AD mice (Lee et al., 2010). A recent study in transgenic AD rats reported increased CX3CL1 along with increased IL1β, TNFα, and COX2 even in young animals (Hanzel et al., 2014). The authors of that study proposed that release of CX3CL1 or other factors by Aβ-damaged neurons could exacerbate or even possibly trigger the inflammatory response in the AD brain.

While it seems obvious that age-related and Aβ-related damage to neurons would contribute to a neurodegenerative process, age is not the sole cause of AD and neither is Aβ since Aβ accumulation in brain is frequently observed in aged individuals who show little or no dementia (Lee et al., 2004; Castellani et al., 2009). It is likely that factors in addition to age and Aβ can push the brain into a neurodegenerative state. In this study, that factor is LPS, which is meant to represent the kind of debris the builds up from a lifetime of fighting bacterial infections. Such debris can persist as an inflammatory stimulus and invade the aged and AD brain (Miklossy, 2008; Bibi et al., 2014).

Experimental evidence indicates that young and old microglia exposed to Aβ alone (i.e., without LPS) take on similar phenotypes except for phagocytosis. Specifically, both young and old microglia exposed to Aβ have increased production of ROS and of pro- and anti-inflammatory mediators (except for decreased production of IGF1), but young microglia have increased phagocytosis while old microglia have decreased phagocytosis (for references see Anastasio, 2014). When old microglia are exposed to Aβ and LPS together *in vitro* they also have increased production of ROS and of pro-inflammatory cytokines and decreased phagocytosis, but with Aβ and LPS together old microglia have *decreased* production of anti-inflammatory mediators (including IGF1) (Piazza and Lynch, 2009). Deprived of whatever protection the anti-inflammatory mediators may offer (see below), this phenotype is considered neurotoxic. It has not been described *in vivo* but is here conjectured to occur in aged and AD brains, due to the possible infiltration of inflammatory stimuli besides Aβ (such as LPS) that can also activate the TLR complex. The computational drug-combination screen presented here took this neurotoxic phenotype, as initiated by a combination of Aβ and LPS in old microglia, as a starting point, but only some of the findings are dependent on LPS.

The neurotoxic phenotype simulated here is triggered in the old case by `Ab` and `LPS` together, signaling through `TLR4`, but is produced and maintained by a transcription-factor pattern in which `NFkB` is expressed at its highest level while `PPARg` is expressed at its lowest level. All seven of the synergistically efficacious drug combinations work by reversing that pattern, in part or in whole. The seven efficacious combinations involve six of the ten drugs: `aura`, `glim`, `ibup`, `nalo`, `nico`, and `rosi`. Of those, only `nalo` works by blocking activation of `TLR4` by `LPS` (and `Ab`). All of the others (except `nico`) work on elements that more directly determine the levels of `NFkB` and `PPARg` (see Results). If, as conjectured here, a neurotoxic phenotype occurs in the aged and AD brain because of co-stimulation by Aβ and other TLR4 ligands (such as LPS), then the model suggests that drug combinations that include a TLR4 blocker, such as the non-opioid form of naloxone, would help to reduce that neurotoxicity (opioid forms that block both TLR2 and TLR4 might help even more). If, on the other hand, AD does not involve co-stimulation between Aβ and other TLR ligands, then the neurotoxic phenotype described here can be considered as a worst-case scenario of microglial activation. In that case the model suggests that certain combinations of auranofin, glimepiride, ibuprofen, and rosiglitazone would help to reduce microglial inflammation in AD. It further suggests that nicotine can contribute by reducing ROS in some of those combinations.

The two most efficacious combinations were `glim/ibup` and `glim/ibup/nico`. The combined effects of `glim` and `ibup` were enough to completely reverse the neurotoxic transcriptional pattern involving `NFkB` and `PPARg`, resulting in `low` expression of pro-inflammatory cytokines, `high` expression of anti-inflammatory mediators including `IGF1`, and `high` `phago`. Reduction of `ROS` from `base` to `low` by the addition of `nico` completed the conversion from the fully neurotoxic to the fully neuroprotective phenotype. Among the anti-inflammatory factors expressed at a `high` level in the neuroprotective phenotype is `TGFb` (see Results). Various mechanisms of neuroprotection by TGFβ through direct action on neurons have been described (for review see Caraci et al., 2012). It is possible that certain anti-inflammatory mediators including IL4 and IGF1 may also be neuroprotective via mechanisms that go beyond suppression of the neurotoxic microglial state.

Two further aspects of the highly efficacious `glim`/`ibup` and `glim`/`ibup`/`nico` combinations stand out. First, only combinations including both `glim` and `ibup` were able completely to reverse the neurotoxic `NFkB`–`PPARg` pattern. Second, only combinations including both `glim` and `ibup` were associated with only one stable state. These two aspects are related.

The neuroprotective transcriptional pattern (`NFkB low` but `PPARg high`) can be maintained only when `IGF1` is able to sustain its own `high` expression though activation of the `Gq` pathway. This mechanism is tenuous because it cannot be maintained through synergism with other anti-inflammatory mediators but can only be sustained by `IGF1` itself (see Subsection Microglia Model Behavior). The efficacious drug combinations that did not include both `glim` and `ibup` could not completely reverse the neurotoxic `NFkB`–`PPARg` pattern, nor could they even guarantee, for all orders of updates of the autocrine receptors (i.e., all state trajectories), that the partial reversal they could produce would be maintained. Thus, the `glim`/`ibup` and the `glim`/`ibup`/`nico` combinations emerge from the analysis as the most efficacious as well as the most reliable. The model suggests that the combination of glimepiride and ibuprofen could effectively and reliably reduce microglial inflammation in AD, and could also reduce ROS with the addition of nicotine.

The impetus for the computational drug-combination screen described here is similar to that which drives other computational and experimental approaches in the emerging area of polypharmacology (Keith et al., 2005; Hopkins, 2008; Lehar et al., 2009; Xie et al., 2012). What sets this computational study apart is its use of both imperative and declarative programming modalities to simulate and analyze a pathological system. This dual approach allows both identification of potentially effective drug combinations and detailed analysis of their putative mechanisms of action. As such, the model generates predictions of both therapeutic and basic-science relevance.

The most direct way to test the specific predictions generated here would be to use old microglia exposed to both Aβ and LPS *in vitro* (for *in vitro* experiments, insulin itself would be used in place of glimepiride). Validation *in vitro* that the efficacious drug combinations identified here actually do reduce microglial inflammation would provide strong justification for *in vivo* tests, which could lead to clinical trials. However, failure to validate model predictions would also be useful, and in that case the ability to use declarative analysis tools is critical. While descriptions of the mechanisms of action of the various drug combinations may seem tedious they are nevertheless essential, because if the predictions are not validated, then experiments involving the receptors, signaling molecules, transcription factors, and other elements can show us specifically where the model goes wrong and how to correct it. Yoking computational and experimental efforts would spur development of a model of ever increasing explanatory power, and one that would produce increasingly valuable predictions concerning multi-drug therapies aimed at the highly complex and severely damaging inflammatory component of neurodegenerative diseases including AD.

References

Anastasio, T. J. (2014). Temporal-logic analysis of microglial phenotypic conversion with exposure to amyloid-β. *Mol. Biosyst.* 11, 434–453. doi: 10.1039/C4MB00457D

Armstrong, R. A. (2014). A critical analysis of the 'amyloid cascade hypothesis'. *Folia Neuropathol.* 52, 211–225. doi: 10.5114/fn.2014.45562

Bibi, F., Yasir, M., Sohrab, S. S., Azhar, E. I., Al-Qahtani, M. H., Abuzenadah, A. M., et al. (2014). Link between chronic bacterial inflammation and Alzheimer disease. *CNS Neurol. Disord. Drug Targets* 13, 1140–1147. doi: 10.2174/1871527313666140917115741

Butovsky, O., Talpalar, A. E., Ben-Yaakov, K., and Schwartz, M. (2005). Activation of microglia by aggregated β-amyloid or lipopolysaccharide impairs MHC-II expression and renders them cytotoxic whereas IFN-gamma and IL-4 render them protective. *Mol. Cell. Neurosci.* 29, 381–393. doi: 10.1016/j.mcn.2005.03.005

Campbell, R. K. (1998). Glimepiride: role of a new sulfonylurea in the treatment of type 2 diabetes mellitus. *Ann. Pharmacother.* 32, 1044–1052. doi: 10.1345/aph.17360

Caraci, F., Spampinato, S., Sortino, M. A., Bosco, P., Battaglia, G., Bruno, V., et al. (2012). Dysfunction of TGF-β1 signaling in Alzheimer's disease: perspectives for neuroprotection. *Cell Tissue Res.* 347, 291–301. doi: 10.1007/s00441-011-1230-6

Cardona, A. E., Pioro, E. P., Sasse, M. E., Kostenko, V., Cardona, S. M., Dijkstra, I. M., et al. (2006). Control of microglial neurotoxicity by the fractalkine receptor. *Nat. Neurosci.* 9, 917–924. doi: 10.1038/nn1715

Castellani, R. J., Lee, H. G., Siedlak, S. L., Nunomura, A., Hayashi, T., Nakamura, M., et al. (2009). Reexamining Alzheimer's disease: evidence for a protective role for amyloid-β protein precursor and amyloid-β. *J. Alzheimers Dis.* 18, 447–452. doi: 10.3233/JAD-2009-1151

Clavel, M., Durán, R., Eker, S., Lincoln, P., Martí-Oliet, N., Meseguer, J., et al. (2007). *All About Maude—A High-Performance Logical Framework: How to Specify, Program, and Verify Systems in Rewriting Logic.* Berlin: Springer.

Combs, C. K., Johnson, D. E., Cannady, S. B., Lehman, T. M., and Landreth, G. E. (1999). Identification of microglial signal transduction pathways mediating a neurotoxic response to amyloidogenic fragments of β-amyloid and prion proteins. *J. Neurosci.* 19, 928–939.

De Simone, R., Ajmone-Cat, M. A., Carnevale, D., and Minghetti, L. (2005). Activation of alpha7 nicotinic acetylcholine receptor by nicotine selectively up-regulates cyclooxygenase-2 and prostaglandin E2 in rat microglial cultures. *J. Neuroinflammation* 2:4. doi: 10.1186/1742-2094-2-4

Fang, J., Rhyasen, G., Bolanos, L., Rasch, C., Varney, M., Wunderlich, M., et al. (2012). Cytotoxic effects of bortezomib in myelodysplastic syndrome/acute myeloid leukemia depend on autophagy-mediated lysosomal degradation of TRAF6 and repression of PSMA1. *Blood* 120, 858–867. doi: 10.1182/blood-2012-02-407999

Fernandez, A. M., and Torres-Aleman, I. (2012). The many faces of insulin-like peptide signalling in the brain. *Nat. Rev. Neurosci.* 13, 225–239. doi: 10.1038/nrn3209

Fisher, J., and Henzinger, T. A. (2007). Executable cell biology. *Nat. Biotechnol.* 25, 1239–1249. doi: 10.1038/nbt1356

Griffin, W. S., and Mrak, R. E. (2002). Interleukin-1 in the genesis and progression of and risk for development of neuronal degeneration in Alzheimer's disease. *J. Leukoc. Biol.* 72, 233–238.

Hanzel, C. E., Pichet-Binette, A., Pimentel, L. S., Iulita, M. F., Allard, S., Ducatenzeiler, A., et al. (2014). Neuronal driven pre-plaque inflammation in a transgenic rat model of Alzheimer's disease. *Neurobiol. Aging* 35, 2249–2262. doi: 10.1016/j.neurobiolaging.2014.03.026

Hardy, J., Bogdanovic, N., Winblad, B., Portelius, E., Andreasen, N., Cedazo-Minguez, A., et al. (2014). Pathways to Alzheimer's disease. *J. Intern. Med.* 275, 296–303. doi: 10.1111/joim.12192

Hardy, J., and Selkoe, D. J. (2002). The amyloid hypothesis of Alzheimer's disease: progress and problems on the road to therapeutics. *Science* 297, 353–356. doi: 10.1126/science.1072994

Hopkins, A. L. (2008). Network pharmacology: the next paradigm in drug discovery. *Nat. Chem. Biol.* 4, 682–690. doi: 10.1038/nchembio.118

Hutchinson, M. R., Zhang, Y., Brown, K., Coats, B. D., Shridhar, M., Sholar, P. W., et al. (2008). Non-stereoselective reversal of neuropathic pain by naloxone and naltrexone: involvement of toll-like receptor 4 (TLR4). *Eur. J. Neurosci.* 28, 20–29. doi: 10.1111/j.1460-9568.2008.06321.x

Huth, M., and Ryan, M. (2004). *Logic in Computer Science: Modelling and Reasoning about Systems*. Cambridge: Cambridge University Press.

Ingham, V., Williams, A., and Bate, C. (2014). Glimepiride reduces CD14 expression and cytokine secretion from macrophages. *J. Neuroinflammation* 11:115. doi: 10.1186/1742-2094-11-115

Jeon, K. I., Byun, M. S., and Jue, D. M. (2003). Gold compound auranofin inhibits IkappaB kinase (IKK) by modifying Cys-179 of IKKβ subunit. *Exp. Mol. Med.* 35, 61–66. doi: 10.1038/emm.2003.9

Jeon, K. I., Jeong, J. Y., and Jue, D. M. (2000). Thiol-reactive metal compounds inhibit NF-kappa B activation by blocking I kappa B kinase. *J. Immunol.* 164, 5981–5989. doi: 10.4049/jimmunol.164.11.5981

Johnston, H., Boutin, H., and Allan, S. M. (2011). Assessing the contribution of inflammation in models of Alzheimer's disease. *Biochem. Soc. Trans.* 39, 886–890. doi: 10.1042/BST0390886

Keith, C. T., Borisy, A. A., and Stockwell, B. R. (2005). Multicomponent therapeutics for networked systems. *Nat. Rev. Drug Discov.* 4, 71–78. doi: 10.1038/nrd1609

Kettenmann, H., Hanisch, U. K., Noda, M., and Verkhratsky, A. (2011). Physiology of microglia. *Physiol. Rev.* 91, 461–553. doi: 10.1152/physrev.00011.2010

Koenigsknecht-Talboo, J., and Landreth, G. E. (2005). Microglial phagocytosis induced by fibrillar β-amyloid and IgGs are differentially regulated by proinflammatory cytokines. *J. Neurosci.* 25, 8240–8249. doi: 10.1523/JNEUROSCI.1808-05.2005

Lawasut, P., Chauhan, D., Laubach, J., Hayes, C., Fabre, C., Maglio, M., et al. (2012). New proteasome inhibitors in myeloma. *Curr. Hematol. Malig. Rep.* 7, 258–266. doi: 10.1007/s11899-012-0141-2

Lee, H. G., Casadesus, G., Zhu, X., Takeda, A., Perry, G., and Smith, M. A. (2004). Challenging the amyloid cascade hypothesis: senile plaques and amyloid-β as protective adaptations to Alzheimer disease. *Ann. N.Y. Acad. Sci.* 1019, 1–4. doi: 10.1196/annals.1297.001

Lee, S., Varvel, N. H., Konerth, M. E., Xu, G., Cardona, A. E., Ransohoff, R. M., et al. (2010). CX3CR1 deficiency alters microglial activation and reduces β-amyloid deposition in two Alzheimer's disease mouse models. *Am. J. Pathol.* 177, 2549–2562. doi: 10.2353/ajpath.2010.100265

Lehar, J., Krueger, A. S., Avery, W., Heilbut, A. M., Johansen, L. M., Price, E. R., et al. (2009). Synergistic drug combinations tend to improve therapeutically relevant selectivity. *Nat. Biotechnol.* 27, 659–666. doi: 10.1038/nbt.1549

Lewis, S. S., Loram, L. C., Hutchinson, M. R., Li, C. M., Zhang, Y., Maier, S. F., et al. (2012). (+)-naloxone, an opioid-inactive toll-like receptor 4 signaling inhibitor, reverses multiple models of chronic neuropathic pain in rats. *J. Pain* 13, 498–506. doi: 10.1016/j.jpain.2012.02.005

Lim, G. P., Yang, F., Chu, T., Chen, P., Beech, W., Teter, B., et al. (2000). Ibuprofen suppresses plaque pathology and inflammation in a mouse model for Alzheimer's disease. *J. Neurosci.* 20, 5709–5714.

Loane, D. J., Deighan, B. F., Clarke, R. M., Griffin, R. J., Lynch, A. M., and Lynch, M. A. (2009). Interleukin-4 mediates the neuroprotective effects of rosiglitazone in the aged brain. *Neurobiol. Aging* 30, 920–931. doi: 10.1016/j.neurobiolaging.2007.09.001

Mandrekar-Colucci, S., and Landreth, G. E. (2010). Microglia and inflammation in Alzheimer's disease. *CNS Neurol. Disord. Drug Targets* 9, 156–167. doi: 10.2174/187152710791012071

Matthews, S. J., and McCoy, C. (2003). Thalidomide: a review of approved and investigational uses. *Clin. Ther.* 25, 342–395. doi: 10.1016/S0149-2918(03)80085-1

McDonald, D. R., Brunden, K. R., and Landreth, G. E. (1997). Amyloid fibrils activate tyrosine kinase-dependent signaling and superoxide production in microglia. *J. Neurosci.* 17, 2284–2294.

Miklossy, J. (2008). Chronic inflammation and amyloidogenesis in Alzheimer's disease—role of Spirochetes. *J. Alzheimers Dis.* 13, 381–391.

Moon, J. H., Kim, S. Y., Lee, H. G., Kim, S. U., and Lee, Y. B. (2008). Activation of nicotinic acetylcholine receptor prevents the production of reactive oxygen species in fibrillar β amyloid peptide (1-42)-stimulated microglia. *Exp. Mol. Med.* 40, 11–18. doi: 10.3858/emm.2008.40.1.11

Nam, S., Williams, A., Vultur, A., List, A., Bhalla, K., Smith, D., et al. (2007). Dasatinib (BMS-354825) inhibits Stat5 signaling associated with apoptosis in chronic myelogenous leukemia cells. *Mol. Cancer Ther.* 6, 1400–1405. doi: 10.1158/1535-7163.MCT-06-0446

Necela, B. M., Su, W., and Thompson, E. A. (2008). Toll-like receptor 4 mediates cross-talk between peroxisome proliferator-activated receptor gamma and nuclear factor-kappaB in macrophages. *Immunology* 125, 344–358. doi: 10.1111/j.1365-2567.2008.02849.x

Noman, A. S., Koide, N., Hassan, F., E-Khuda, I. I., Dagvadorj, J., Tumurkhuu, G., et al. (2009). Thalidomide inhibits lipopolysaccharide-induced tumor necrosis factor-alpha production via down-regulation of MyD88 expression. *Innate Immun.* 15, 33–41. doi: 10.1177/1753425908099317

Park, B. S., Song, D. H., Kim, H. M., Choi, B. S., Lee, H., and Lee, J. O. (2009). The structural basis of lipopolysaccharide recognition by the TLR4-MD-2 complex. *Nature* 458, 1191–1195. doi: 10.1038/nature07830

Piazza, A., and Lynch, M. A. (2009). Neuroinflammatory changes increase the impact of stressors on neuronal function. *Biochem. Soc. Trans.* 37, 303–307. doi: 10.1042/BST0370303

Ransohoff, R. M., and Perry, V. H. (2009). Microglial physiology: unique stimuli, specialized responses. *Annu. Rev. Immunol.* 27, 119–145. doi: 10.1146/annurev.immunol.021908.132528

Reed-Geaghan, E. G., Savage, J. C., Hise, A. G., and Landreth, G. E. (2009). CD14 and toll-like receptors 2 and 4 are required for fibrillar A{β}-stimulated microglial activation. *J. Neurosci.* 29, 11982–11992. doi: 10.1523/JNEUROSCI.3158-09.2009

Reitz, C. (2012). Alzheimer's disease and the amyloid cascade hypothesis: a critical review. *Int. J. Alzheimers Dis.* 2012, 369808. doi: 10.1155/2012/369808

Shytle, R. D., Mori, T., Townsend, K., Vendrame, M., Sun, N., Zeng, J., et al. (2004). Cholinergic modulation of microglial activation by alpha 7 nicotinic receptors. *J. Neurochem.* 89, 337–343. doi: 10.1046/j.1471-4159.2004.02347.x

Skaper, S. D. (2012). Alzheimer's disease and amyloid: culprit or coincidence? *Int. Rev. Neurobiol.* 102, 277–316. doi: 10.1016/b978-0-12-386986-9.00011-9

Smith, K., Hopp, M., Mundin, G., Bond, S., Bailey, P., Woodward, J., et al. (2012). Low absolute bioavailability of oral naloxone in healthy subjects. *Int. J. Clin. Pharmacol. Ther.* 50, 360–367. doi: 10.5414/CP201646

Sung, S., Yang, H., Uryu, K., Lee, E. B., Zhao, L., Shineman, D., et al. (2004). Modulation of nuclear factor-kappa B activity by indomethacin influences A β levels but not A β precursor protein metabolism in a model of Alzheimer's disease. *Am. J. Pathol.* 165, 2197–2206. doi: 10.1016/S0002-9440(10)63269-5

Verstovsek, S. (2013). Ruxolitinib: an oral Janus kinase 1 and Janus kinase 2 inhibitor in the management of myelofibrosis. *Postgrad. Med.* 125, 128–135. doi: 10.3810/pgm.2013.01.2628

Von Bernhardi, R. (2007). Glial cell dysregulation: a new perspective on Alzheimer disease. *Neurotox. Res.* 12, 215–232. doi: 10.1007/BF03033906

Wang, L., Xu, Y. L., and Zhang, X. Q. (2014). Bortezomib in combination with thalidomide or lenalidomide or doxorubicin regimens for the treatment of multiple myeloma: a meta-analysis of 14 randomized controlled trials. *Leuk. Lymphoma* 55, 1479–1488. doi: 10.3109/10428194.2013.838232

Wilkinson, B., Koenigsknecht-Talboo, J., Grommes, C., Lee, C. Y., and Landreth, G. (2006). Fibrillar β-amyloid-stimulated intracellular signaling cascades require Vav for induction of respiratory burst and phagocytosis in monocytes and microglia. *J. Biol. Chem.* 281, 20842–20850. doi: 10.1074/jbc.M600627200

Wong, W. T. (2013). Microglial aging in the healthy CNS: phenotypes, drivers, and rejuvenation. *Front. Cell. Neurosci.* 7:22. doi: 10.3389/fncel.2013.00022

Xie, L., Xie, L., Kinnings, S. L., and Bourne, P. E. (2012). Novel computational approaches to polypharmacology as a means to define responses to individual

drugs. *Annu. Rev. Pharmacol. Toxicol.* 52, 361–379. doi: 10.1146/annurev-pharmtox-010611-134630

Yan, Q., Zhang, J., Liu, H., Babu-Khan, S., Vassar, R., Biere, A. L., et al. (2003). Anti-inflammatory drug therapy alters β-amyloid processing and deposition in an animal model of Alzheimer's disease. *J. Neurosci.* 23, 7504–7509.

Yarilina, A., Xu, K., Chan, C., and Ivashkiv, L. B. (2012). Regulation of inflammatory responses in tumor necrosis factor-activated and rheumatoid arthritis synovial macrophages by JAK inhibitors. *Arthritis Rheum.* 64, 3856–3866. doi: 10.1002/art.37691

Conflict of Interest Statement: The author declares that the research was conducted in the absence of any commercial or financial relationships that could be construed as a potential conflict of interest.